Electronic Supplementary Material (ESI) for Physical Chemistry Chemical Physics.

A Coarse-Grained Model for Mechanical Behavior of Phosphorene Sheet

Ning Liu[1], Mathew Becton[1], Liuyang Zhang[2], Heng Chen[3], Xiaowei Zeng[4], Ramana Pidaparti[1] and Xianqiao Wang[1*]

[1]College of Engineering, University of Georgia, Athens, GA 30602 USA

[2] State Key Laboratory for Manufacturing Systems Engineering, Xi'an Jiaotong University, Xi'an, Shaanxi, 710049, China

[3]College of Astronautics, Nanjing University of Aeronautics and Astronautics, Nanjing, 210016, China

[4]Department of Mechanical Engineering, University of Texas at San Antonio, San Antonio, TX 78249 USA

[*]Corresponding author: xqwang@uga.edu

1. Angle variation in deformation

As shown in Figure S1 (a), Angle θ, involving two bonds jointed by bead *b*, changes along with the rotation of bond *ab*, when bond *cb* is fixed. Note that the rotation plane is not the same as the plane defined by bead *a*, *b* and *c*. In this case, the variation of angle θ can be expressed as a function of angle α, the angle between rotation plane and fixed bond *cb*, and angle β, the angle between projection of bond *cb* onto rotation plane and bond *ab*. Mathematically, the relation can be expressed as follows,

$$cos\theta = cos\alpha * cos\beta \quad \text{(S1).}$$

As we take differentials on both sides assuming that angle α maintains the same during rotation of bond *cb*, we can get the following equation

$$\delta\theta = \frac{cos\alpha * sin\beta}{sin\theta}\delta\beta \quad \text{(S2)}$$

Figure S1 (b)-(d) shows the change of angle θ_1 and θ_2 under uniaxial tension along armchair direction, while Figure S2 shows angle changes under uniaxial tension along zigzag direction.

2. Force-displacement relation analysis for a unit cell

Figure S3 shows the force and deformation map of a unit cell under uniaxial tension along both armchair and zigzag direction. In this case, Bead B_2 is assumed to be fixed while the other beads can translate along bond direction and rotate around bead B_2. Figure S2(a) shows the free body diagram under uniaxial tension along armchair direction. Under the forces shown in Figure S2(a), the beads would move coordinately and thus the unit cell would deform as shown in Figure S2(b). The movement of beads can be decomposed into two parts: translation along the bond direction and rotation around the fixed bead B_2. The translation can be calculated through dividing the force component along bond direction by the bond stiffness. However, the rotation is a little bit complicated, in which all the angle springs involving the targeted beads should be taken into consideration. In other words, the effect of angle network can not be neglected. Take bead B_4 in Figure S3(b) for example, the translation along bond B_2-B_4 can be easily calculated by dividing the force component along B_2-B_4, $2Fcos30.6^0$, by the stiffness of bond B_2-B_4, k_b. On the other hand, for bead B_4, there are four θ_2 angles would change identically due to the torque generated by the force on bead B_4. Therefore, the rotation of should be calculated by the following expression, $r_2 \frac{2Fsin30.6^0 r_2}{4k_{\theta_2}c_3}$, where r_2 is the length of bond B_2-B_4, k_{θ_2} is the stiffness of angle θ_2, and c_3 is the ratio between variation of θ_2, $\delta\theta_2$, and the variation of β_2, $\delta\beta_2$, as shown in Figure S1(d). Similarly, the movement of the other beads can be calculated.

Subsequently, the elastic modulus can be calculated under uniaxial tension along both x (armchair) and y (zigzag) direction. First, the strain along x direction can be expressed as follows:

$$\varepsilon_x = \frac{d_x}{\frac{a_1}{2}} = \frac{\frac{Fsin79.8^0 {r_1}^2}{2k_\theta c_1 + 2k_\theta c_2} sin79.8^0 + \frac{Fcos79.8^0}{k_b} cos79.8^0 + \frac{2Fsin30.6^0 r_2^2}{4k_\theta c_3} sin30.6^0 + \frac{2Fcos30.6^0}{k_b} cos30.6^0}{\frac{a_1}{2}} \quad \text{(S3)}$$

where a_1 is the lattice constant along x (armchair) direction as shown in Figure 1(a).The stress along x direction can be expressed as follows:

$$\sigma_x = \frac{2F}{ha_2} \tag{S4}$$

where h is the interlayer distance as shown in Figure 1(d) while a_2 is the lattice constant along y (zigzag direction) as shown in Figure 1(a). Second, the strain along the y direction can be expressed as follows:

$$\varepsilon_y = \frac{d_y}{a_2} = \frac{2\frac{Fsin32.9^0 {r_1}^2}{4k_\theta c_4} sin32.9^0 + 2\frac{Fcos32.9^0}{k_b} cos32.9^0}{a_2} \tag{S5}$$

The stress along y direction can be expressed as follows:

$$\sigma_y = \frac{F}{\frac{a_1}{2}h} \tag{S6}$$

Finally, the elastic moduli on both armchair and zigzag direction can be obtained as follows:

$$E_{arm} = \frac{\sigma_x}{\varepsilon_x} \tag{S7}$$

$$E_{zig} = \frac{\sigma_y}{\varepsilon_y} \tag{S8}$$

3. Adhesion energy

Two CG-MD phosphorene sheets sized 344.8 Å×276.8 Å are staggered together with a interlayer distance 5.24 Å as shown in Figure S4(a). During the simulation, the bottom sheet is fixed while the top sheet is moved stepwise with step size 8 Å following energy minimization, in which periodic boundary conditions are adopted in x and y direction while non-periodic boundary condition is applied in z direction. A set of simulations have been done, in which potential well ε for Lennard-Jones potential is tuned to approach the targeted interlayer adhesion for phosphorene systems. An example of potential energy change with the potential well ε equal to 0.167eV is shown in Figure S(4)b, indicating that when D is bigger than 8 Å the potential energy change compared to equilibrium state reaches a plateau. This potential energy change determines the work done to separate two phosphorene sheets. Accordingly, the resultant interlayer adhesion γ_{ad} is equal to 0.345 J/m^2, in close agreement with our targeted adhesion for phosphorene. The optimized value for ε is equal to 0.167 eV as listed in Table 1. The other parameter σ = 4.45 Å listed in Table 1 is obtained to ensure that the interlayer distance h is equal to 5.24 Å as shown in Figure 1(d) [2, 3]. We include associated revisions in section 2.2 in the main context.

Figures

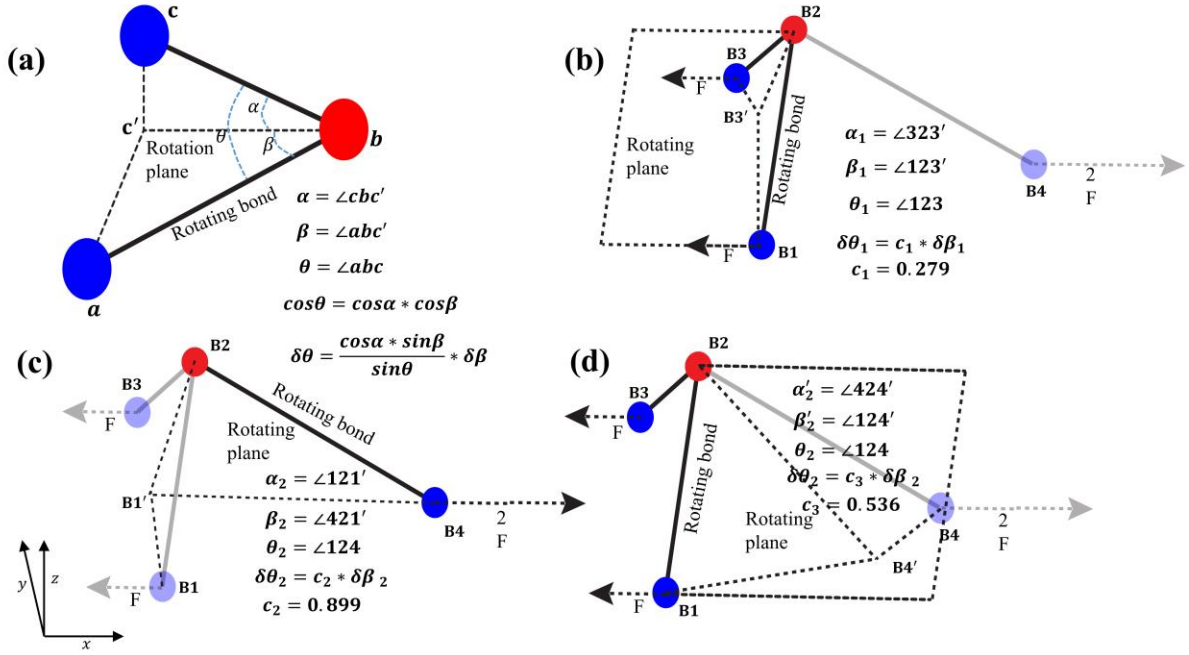

Figure S1 The relations between rotation angle of bonds and the change of angle springs under uniaxial tension along armchair direction.

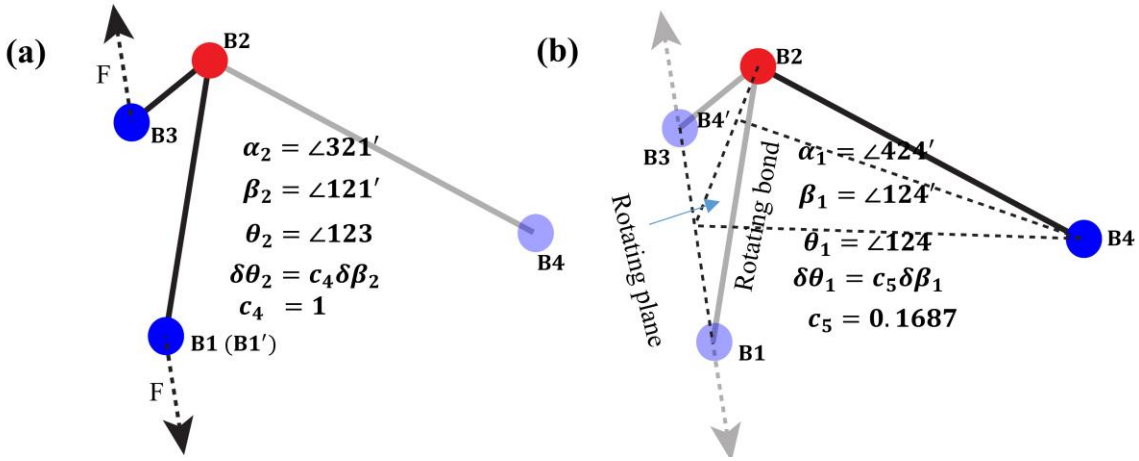

Figure S2 The relations between rotation angle of bonds and the change of angle springs under uniaxial tension along zigzag direction.

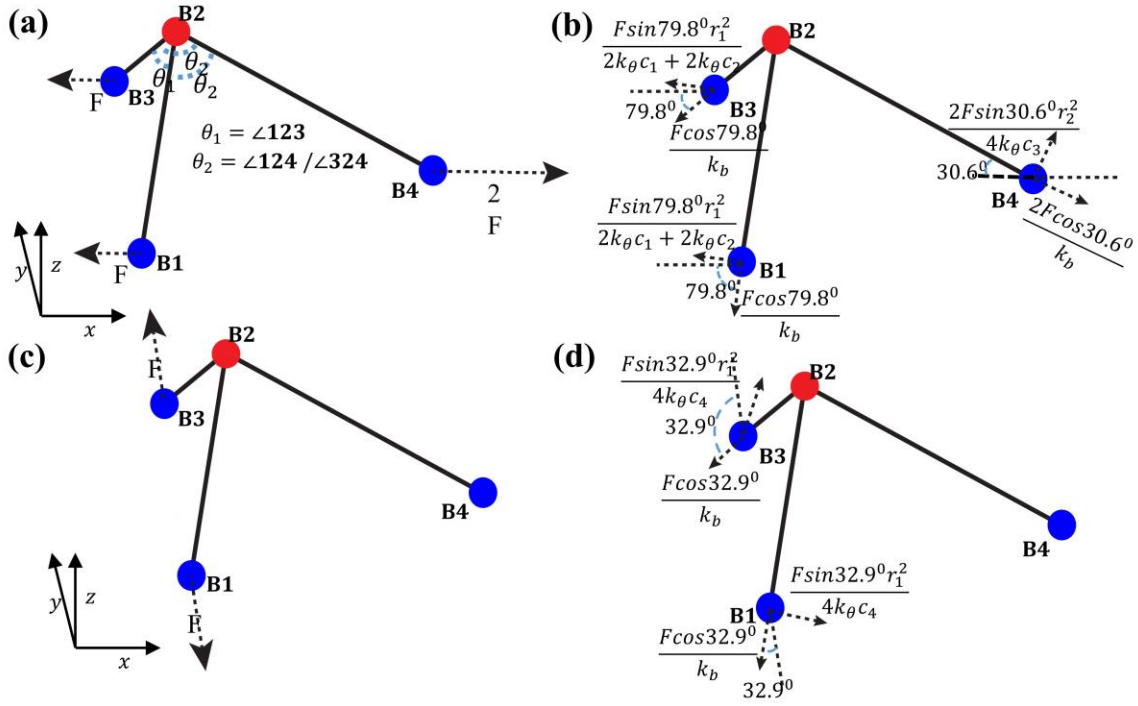

Figure S3 Force-displacement map of a unit cell under uniaxial tension along both armchair and zigzag directions.

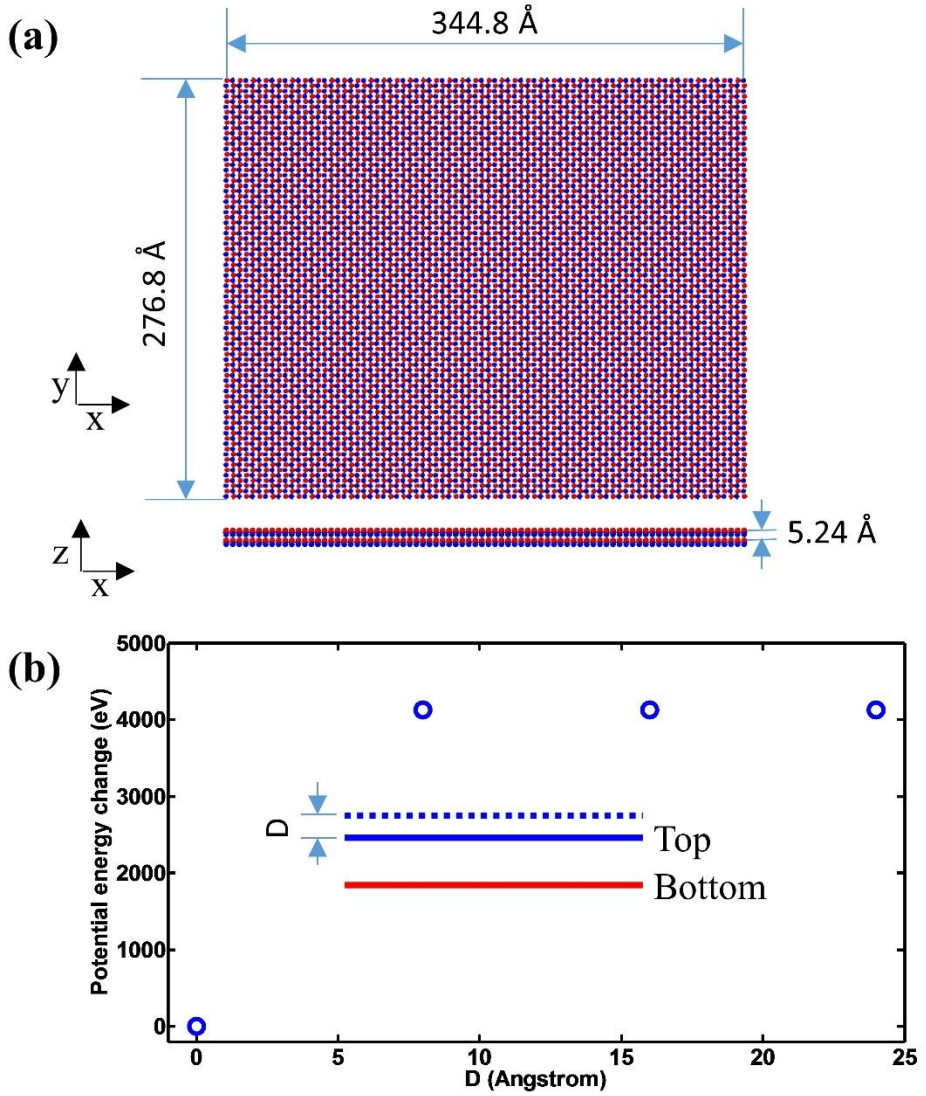

Figure S4. (a) Top view of the simulated phosphorene sheets; (b) Potential energy change during the separation of two adjacent phosphorene sheets (inset shows schematically how the separation of two phosphorene sheets is done, in which the bottom sheet is fixed while the distance between top and bottom sheet can be tuned).

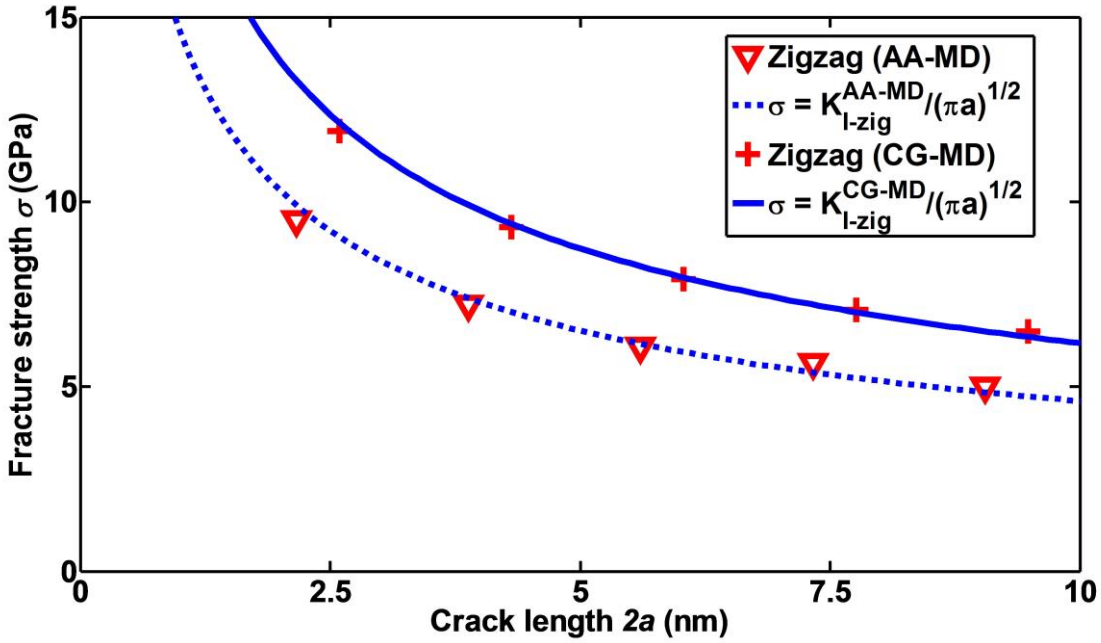

Figure S5 Fracture strength versus crack length for phosphorene sheets with cracks vertical to the zigzag direction under tension along zigzag direction